PROTEINS
STRUCTURE ■ FUNCTION ■ BIOINFORMATICS

Characterization of cancer-linked BRCA1-BRCT missense variants and their interaction with phosphoprotein targets

Ioannis Drikos,[1] George Nounesis,[2] and Constantinos E. Vorgias[1]*

[1] Department of Biochemistry and Molecular Biology, Faculty of Biology, National and Kapodistrian University of Athens, Panepistimiopolis-Zographou, 15701 Athens, Hellas

[2] Biomolecular Physics Laboratory, IRRP, National Centre for Scientific Research "Demokritos", 15310 Aghia Paraskevi, Hellas

ABSTRACT

The breast cancer tumor suppressor protein BRCA1 is involved in DNA repair and cell cycle control. Mutations at the two C-terminal tandem (BRCT) repeats of BRCA1 detected in breast tumor patients were identified either to lower the stability of the BRCT domain and/or to disrupt the interaction of BRCT with phoshpopeptides. The aim of this study was to analyze five BRCT pathogenic mutations for their effect on structural integrity and protein stability. For this purpose, the five cancer-associated BRCT mutants: V1696L, M1775K, M1783T, V1809F, and P1812A were cloned in suitable prokaryotic protein production vectors, and the recombinant proteins were purified in soluble and stable form for further biophysical studies. The biophysical analysis of the secondary structure and the thermodynamic stability of the wild-type, wt, and the five mutants of the BRCT domain were performed by Circular Dichroism Spectroscopy (CD) and Differential Scanning Microcalorimetry (DSC), respectively. The binding capacity of the wt and mutant BRCT with (pBACH1/BRIP1) and pCtIP were measured by Isothermal Titration Calorimetry (ITC). The experimental results demonstrated that the five mutations of the BRCT domain: (i) affected the thermal unfolding temperature as well as the unfolding enthalpy of the domain, to a varying degree depending upon the induced destabilization and (ii) altered and/or abolished their affinity to synthetic pBACH1/BRIP1 and pCtIP phosphopeptides by affecting the structural integrity of the BRCT active sites. The presented experimental results are one step towards the elucidation of the effect of various missense mutations on the structure and function of BRCA1-BRCT.

Proteins 2009; 77:464–476.

Key words: breast cancer; BRCA1-BRCT; pCtIP; pBACH1/BRIP1; mutations; CD; DSC; ITC.

INTRODUCTION

The breast cancer susceptibility gene *brca1* is one of the most well studied genes in cancer research. The BRCA1 protein, 220 kDa, is a tumor suppressor and is involved in multiple cellular functions, such as DNA repair, cell-cycle checkpoint control and transcription. About 5–10% of breast cancer (BC) and ovarian cancer (OC) are hereditary and 30–50% of these are due to mutations in the susceptibility genes, *BRCA1* and *BRCA2*.[1,2] Women who carry *BRCA1* mutations are particularly susceptible to the development of breast or ovarian cancer at an age earlier than 35–40 years old with a probability rate of 45–60% and 20–40%, respectively. Analogously, women who inherited a *BRCA2* mutation present a 25–40% risk of developing breast cancer and a 10–20% risk of developing ovarian cancer.[3–5]

The structure of the carboxyl terminal domain of BRCA1 is comprised of two structurally identical BRCT repeats each containing 90 amino acids. The fold of each repeat consists of a parallel four-stranded β-sheet located at the central part of the domain surrounded by three α-helices (see Fig. 1). The two BRCT repeats fold together in a specific head-to-tail manner, giving rise to the formation of a conserved, almost all-hydrophobic, inter-repeat interface.[6] This structural motif is also present in other proteins, such as 53BP1 and BARD1.[7]

Most cancer-associated *BRCA1* mutations, identified so far, result in the premature translational termination of the protein and influence BRCA1 integrity and operation.[8] A large number of missense mutations are located in BRCT tandem repeats of BRCA1,[9] while only few of them may cause loss of the protein's function, abolition of protein interactions and protein

Additional Supporting Information may be found in the online version of this article.

Grant sponsor: Reinforcement Programme of Human Research Manpower (PENED); Grant number: 03ED375; Grant sponsor: National and Community Funds (25% from the Greek Ministry of Development-General Secretariat of Research and Technology and 75% from E.U.-European Social Fund).

*Correspondence to: Constantinos E. Vorgias, National and Kapodistrian University of Athens, Faculty of Biology, Department of Biochemistry and Molecular Biology, Panepistimiopolis-Zographou, Athens, Hellas 15784. E-mail: cvorgias@biol.uoa.gr.

Received 17 January 2009; Revised 31 March 2009; Accepted 8 April 2009
Published online 20 April 2009 in Wiley InterScience (www.interscience.wiley.com).
DOI: 10.1002/prot.22460

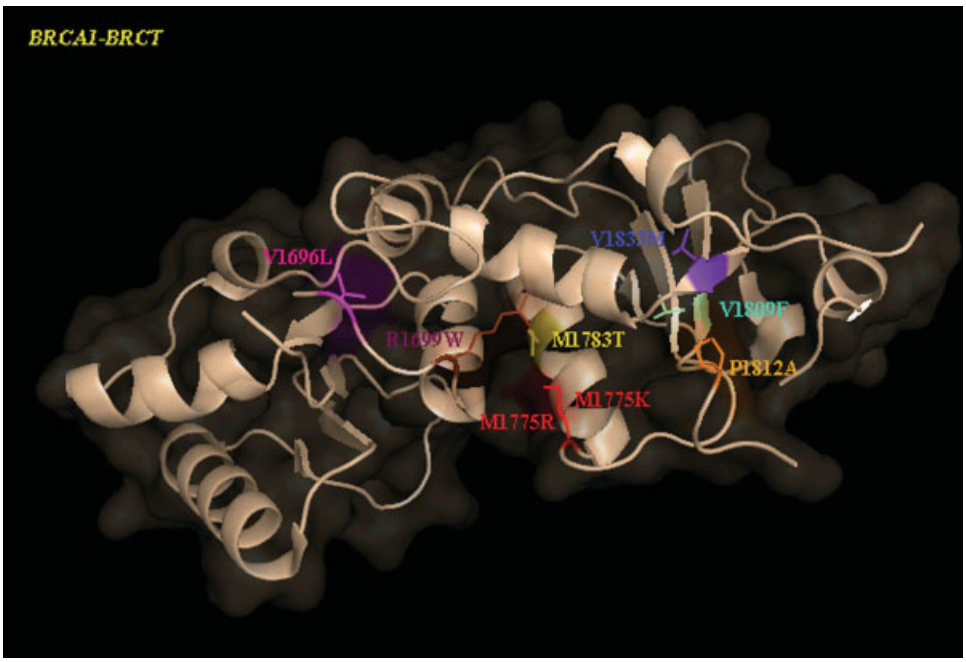

Figure 1

Ribbon representation of the BRCA1-BRCT structure. The positions of the selected mutations have been reported with different colours. M1775K and M1783T are located at the inter-BRCT-repeat interface where the BRCA1-BRCT binding groove for Phe +3 is also located. The exposed V1696L is located at the N-terminal BRCT structural repeat. V1809F, P1812A are found at the C-terminal BRCT repeat. The positions of missense mutations from previously published studies are also depicted. [Color figure can be viewed in the online issue, which is available at www.interscience.wiley.com.]

miss-localization.[10–13] However, their role in BRCT structure and BRCA1 function has not yet been fully elucidated.

The functional and structural integrity of the BRCT tandem repeats is essential for the molecule's interaction with phosphorylated protein targets, such as ACCA, p53, DNA helicase BACH1[14–16] and the CtBP-interacting protein CtIP.[17] The binding of the BRCA1 BRCT domain to BACH1[18,19] and the transcriptional corepressor CtIP play an important role in the control of the G2/M phase checkpoint.[20] Furthermore, BRCT domains of the yeast DNA repair protein Rad9 could bind phosphopeptides, suggesting that the BRCT domains represent a class of ancient phosphopeptide-binding modules.[21]

Potential targets of BRCT domains were identified through database search and structural analysis. Structural analysis of BRCA1-BRCT domain predicted conserved residues that form the phosphopeptide-binding pocket. Thus, the BRCT repeats are a family of phosphopeptide-binding domains in DNA damage responses, highlighting the crucial role for the BRCA1-BRCT domain in mediating BRCA1 tumor suppressor function.[19–22]

The crystal structure of the BRCT complex with the phosphopeptides containing the sequence pSer-X-X-Phe (phosphorylation of Ser990 and Ser327 for the pBACH1/BRIP1 and pCtIP, respectively, and X is for any residue) revealed that phosphoserine is essential for binding.[22–24]

The BRCT domain has been shown to interact with higher affinity to pBACH1/BRIP1 than pCtIP[25] and missense mutations have been proposed to induce the loss of BRCT function by directly altering the binding sites and/or by destabilizing the molecule's overall fold.[26]

The purpose of this study was to analyze five BRCA1-BRCT mutants: V1696L, M1775K, M1783T, V1809F, and P1812A. They were selected because of their reported association with cancer development. Specifically, the study aims at elucidating the influence of those mutations on the domain's binding properties to pBACH1/BRIP1 and pCtIP and at investigating the effects of those mutations on the structural integrity and stability of the BRCT domain.

For this purpose, we cloned and overproduced the BRCT wild type (BRCT-wt) and the five BRCT variants in a highly soluble and stable form. Biophysical analysis of the secondary structure and the thermodynamic stability of the wt and BRCT mutants were evaluated by circular dichroism (CD) and differential scanning microcalorimetry (DSC), respectively. The binding affinity of the wt and BRCT variants with pBACH1/BRIP1 and pCtIP was studied by Isothermal Titration Calorimetry (ITC).

The results presented here clearly show that the studied BRCA1-BRCT mutations (i) influence the thermal stability of the domain and (ii) influence the binding affinities with synthetic pBACH1/BRIP1 and pCtIP pep-

tides. An extensive comparison with previous studies[25] and structural interpretation of the obtained results is discussed.

MATERIALS AND METHODS

Gene cloning and mutagenesis

The encoding region for human wt, the BRCA1 BRCT-tan domain (a.a. 1646-1859) was amplified by PCR using a plasmid kindly provided by Prof. A.N. Monteiro (Cornell University) as template and the following primers: (i) BRCT (*Nde*I), ACATATGGTCAACAAAAGAATGTG-CATGGTG and (ii) BRCT (*Bam*HI), AGGATCCT-CAGGGGATCTGGGGTATCAGG. The primers were designed to build the *Nde*I and *Bam*HI restriction sites at the 5′ and 3′ ends of the *brct* gene fragment (bp 5055–5697 of the *brca1* gene), respectively. The resulting 750 bp PCR product was ligated into the pCR2.1 cloning vector and then transformed into the *E. coli* INVaF′ cells according to the manufacturer's instructions (Invitrogen). The generation of M1783T, M1775K, V1696L, P1812A, and V1809F mutants was carried out using the pCR2.1 cloning vector containing the BRCT coding region of human BRCA1 as the template. The mutations were prepared using the QuickChange site-directed mutagenesis kit (Stratagene) and the primers used are listed in Supporting Information Table 1. Briefly, the PCR products carrying the mutation were digested with *Dpn*I and transformed into the Novablue competent cells (Novagen). Automated DNA sequencing was employed to identify positive clones. The positive clones were digested with *Nde*I and *Bam*HI, and the DNA fragment was then cloned into the pET-3a expression vector (Novagen) and subsequently transformed into the Novablue competent cells. The plasmids isolated from the positive clones were introduced into the *E. coli* BLR(DE3)pLysS expression strain (Novagen).

Protein expression and purification

The BRCT variants P1812A, V1809F, M1783T, M1775K, and V1696L cloned into the pET-3a expression vector were introduced into the *E. coli* BLR(DE3)pLysS strain and were grown at 37°C in LB medium containing 50 m*M* ampicillin and 50 m*M* chloramphenicol to an $OD_{600\ nm}$ of 0.7. Protein overproduction was induced at 24°C for the BRCT-M1783T, BRCT-P1812A mutants, and at 18°C for the BRCT-V1809F, BRCT-M1775K, and BRCT-V1696L mutants, with 0.5 m*M* isopropyl β-D-thiogalactoside (IPTG) for 4–6 h. The bacteria were usually reached the $OD_{600\ nm}$ of 1.6–1.8 and were then harvested by low speed centrifugation in a Sorvall SLA-1500 rotor at 8,000 rpm for 10 min and washed once with ice-cold PBS buffer (10 m*M* Na_2HPO_4, 1.8 m*M* KH_2PO_4, 140 m*M* NaCl, 2.7 m*M* KCl). All further procedures were carried out at 4°C, unless otherwise specified. The bacterial paste was suspended in 10 mL/g buffer A (20 m*M* Na-phosphate pH 6.0, 75 m*M* NaCl, 1 m*M* EDTA, 1 m*M* phenylmethylsulfonyl fluoride (PMSF), 0.5% (w/v) Triton X-100, and 1 m*M* β-mercaptoethanol). The cells were disrupted by sonication (UP200S HIELSCHER ultrasound homogenizer). The extract was centrifuged at 15,000*g* for 25 min, and the soluble protein fraction was applied on a 5 mL SP-Sepharose Fast Flow, previously equilibrated in buffer B (20 m*M* Na-phosphate buffer pH 6.0, 50 m*M* NaCl, 1 m*M* EDTA, 1 m*M* PMSF).

Bound proteins were eluted between 100 and 350 m*M* NaCl of a linear ascending gradient of 50 mL total volume, and 2 mL fractions were collected. Fractions highly enriched in BRCT variants were combined, adjusted to pH 9.0 with buffer C, with fivefold dilution, and applied on a 2 mL Q-Sepharose High Performance column equilibrated in buffer C (5 m*M* Na-borate pH 9.0). Bound proteins were eluted between 100 and 350 m*M* of a linear ascending gradient of 25 mL total volume, and 1 mL fractions were collected. In both cases, the collected fractions were analyzed by 0.1% SDS-15% PAGE Laemmli,[27] using as marker the broad range prestained protein marker (Molecular Probes). The purified mutated BRCT domains are presented in Supporting Information Figure 1.

Table I
Calorimetric Parameters from the DSC Thermograms of BRCT-wt and Mutants M1775K, P1812A, M1783T, V1809F, V1696L, at pH 9.0 (Buffer D) for DSC Heating at a Scan Rate u = 1.5 K/min and Various Protein Concentrations C_t

Mutants	Ct (mg/mL)	T_m (°C)	ΔH (kcal/mol)
BRCT-wt	0.2	48.3 ± 0.5	87.1 ± 6.4
	0.3	48.3 ± 0.5	81.0 ± 6.5
M1775K	0.3	42.1 ± 0.5	85.3 ± 5.0
	0.4	42.1 ± 0.5	89.2 ± 5.0
P1812A	0.2	43.7 ± 0.5	70.0 ± 4.9
	0.3	43.9 ± 0.5	68.0 ± 4.9
	0.4	44.0 ± 0.5	66.9 ± 4.9
M1783T	0.3	40.3 ± 0.5	52.4 ± 4.4
	0.4	40.6 ± 0.5	52.8 ± 4.4
V1809F	0.2	41.9 ± 0.5	69.4 ± 4.9
	0.3	42.1 ± 0.5	71.0 ± 5.0
V1696L	0.2	46.9 ± 0.5	66.2 ± 5.0
	0.3	47.5 ± 0.5	64.0 ± 5.0
M1775R*	0.2	36.7 ± 0.4	43.4 ± 4.2
	0.3	36.3 ± 0.4	44.0 ± 4.2
R1699W*	0.2	40.9 ± 0.5	51.9 ± 4.5
	0.3	40.7 ± 0.5	47.8 ± 4.4
V1833M*	0.3	43.5 ± 0.5	74.0 ± 5.3
	0.4	43.7 ± 0.5	73.5 ± 5.1

The previously published results of M1775R, R1699W, V1833M are also presented for comparison.[25]

Protein detection and verification

Protein analysis was carried out in 0.1% SDS-15% PAGE as described by Laemmli.[27] Protein concentration was determined either by the Bradford method,[28] or

from the molar extinction coefficient at 280 nm. The molar extinction coefficient of BRCT-wt and variants were calculated, from their primary structure, to be 36,440 M^{-1} cm^{-1}.[29,30]

Gel filtration chromatography

Gel filtration chromatography was carried out on a Superose12 HR 10/30 column (Amersham Biosciences). The column was run with an FPLC system at a flow rate of 0.4 mL/min in buffer D (5 m*M* Na-borate pH 9.0, 200 m*M* NaCl). The sample volume loaded each time was 0.2 mL. The absorption (A) of the samples was monitored at 280 nm. All the samples were in the monomer state (Supporting Information Figure 2).

Circular dichroism spectroscopy (CD)

CD measurements were conducted using a JASCO-715 spectropolarimeter equipped with a Peltier type cell holder (PTC-348WI), for temperature control. Wavelength scans in the far (190–260 nm) and near UV region (250–320 nm) were performed in Quartz SUPRASIL (HELLMA) precision cells of 0.1 cm and 1 cm path length, respectively. Each spectrum was obtained by averaging five to eight successive accumulations with a wavelength step of 0.2 nm at a rate of 20 nm/min, response time 1 s and band width 1 nm. Thermal CD experiments were carried out from 20 to 50°C, at 222 nm and heating scan rate 1.5 K/min. In all cases, protein concentrations within the range of 0.5 and 1 mg/mL were used in buffer D.

Differential scanning microcalorimetry (DSC)

Calorimetric measurements were performed on a VP-DSC microcalorimeter (MicroCal) at a heating rate of 1.5 K/min using protein concentrations within the range of 0.2–0.4 mg/mL for P1812A, 0.2, and 0.3 mg/mL for BRCT-wt, V1809F, V1696L, and between 0.3 and 0.4 mg/mL for M1783T, M1775K. All samples were degassed before use and four to five thermal scans, with buffer-filled cells to ensure baseline reproducibility, preceded each sample run. The samples were dissolved in buffer D and were measured twice. A typical DSC experiment consisted of a heating scan at a programmed heating rate followed by a second heating scan to probe the irreversibility of the transitions under study. The difference in the heat capacity between the initial and final states was modeled by a sigmoid chemical baseline.

Isothermal titration calorimetry (ITC)

The interaction of BRCT-wt and the five variants with the BACH1/BRIP1 phosphopeptide ISRSTpSPTFNKQ and the CtIP phosphopeptide PTRVpSSPVFGAT was studied at 20°C in buffer D, using a MCS-ITC calorimeter (Microcal, Northampton). The protein concentration used for the experiments was 0.019 ± 0.003 m*M* and the ligand concentration was 0.21 ± 0.02 m*M*. All ITC experiments were designed as a series of 24 injections, each 10 μL, with 300 s intervals at constant stirring of 400 rpm From the raw exothermic heat pulse data from each injection, the instrumental baseline was subtracted before obtaining normalized integrated heat versus molar ratio data from which the corresponding dilution heat, measured separately for each phosphopeptide, was also subtracted. The ITC experimental data were analyzed via nonlinear least-squares fits of the integrated heat versus molar ratio to single site binding model using ORIGIN. The built-in functions for a single-site binding model providing values for the stoichiometry N, the binding constant K_a and the enthalpy change ΔH. All the ITC control experiments run were repeated at least twice.

Methods in silico

The 1Y98, 1T29, 1JNX, and 1T15 structures and the models of the selected mutants were visualized using the PYMOL software (DeLano Scientific LLC, Palo Alto, CA). Furthermore, the changes of the intermolecular and intramolecular interactions of the mutated residues were analyzed using WHATIF suite (http://swift.cmbi.ru.nl/).

RESULTS

Protein overproduction kinetics for each mutant

The five BRCT variants were prepared and cloned as described in the materials and methods. Protein overproduction kinetic experiments were performed to optimize the culture conditions concerning induction length, growth temperature and solubility of the recombinant proteins. Briefly, the *E. coli* clones containing the M1783T, P1812A BRCT mutants were induced with 0.5 m*M* IPTG at 24°C for 4 h, while the V1809F, M1775K, and V1696L mutants were induced with 0.5 m*M* IPTG at 18°C for 6 h. In all cases, the resulting proteins exhibit high solubility and correct folding compared to the BRCT-wt recombinant protein (see Fig. 2).

Protein purification

A fast and quite reproducible protein purification scheme was developed based on the BRCT-wt purification scheme previously described by our group.[25] After extraction of the recombinant protein and under the mild conditions described in the materials and methods, the soluble protein fraction at low salt conditions was highly enriched in BRCT mutants. A small amount of BRCT was lost due to insolubility.

The purification scheme for all five BRCT mutants was, in principle, the same for each mutant and resulted in an overall yield of about 18 mg of highly purified

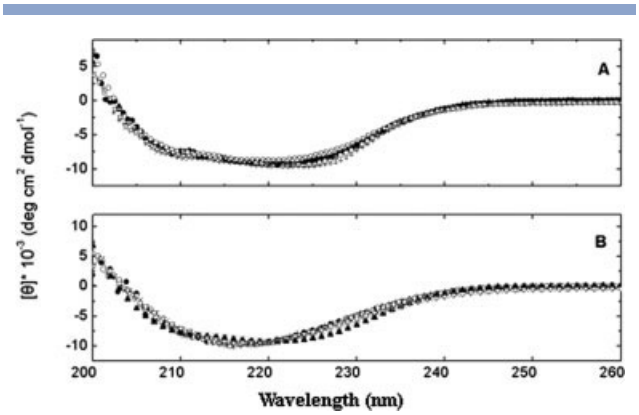

Figure 2

Normalized far-UV CD spectra of BRCT-wt (○), M1775K (●), V1696L (+), P1812A (X), M1783T (--), V1809F (▲) at 25°C. All spectra were carried out at 5 m*M* Na-borate buffer, 200 m*M* NaCl. The missense mutations of the BRCT do not seem to influence the secondary structure of the domain.

BRCT mutant protein (more than 99% pure) from 4 L of bacterial cultures. All purified proteins were verified by Western Blot, using rabbit polyclonal antibody raised against BRCT-wt. Regarding solubility, the purified recombinant proteins BRCT-wt as well as the five mutants of this study are highly soluble and structurally stable for several days at the pH range between 5.5 and 9.5 at 4°C.

Gel filtration chromatography

The monomeric state of the BRCT variants was also verified by high performance gel filtration chromatography in buffer D at 4°C. The results are presented in Supporting Information Figure 2.

Structural features of the six BRCT variants

The five BRCT variants are shown in Figure 1. Both the M1775K and M1783T mutations are located at the hydrophobic interface between the two BRCT repeats formed by the packing of three α-helices. The V1696L mutant is located at the first BRCT repeat, while the V1809F, P1812A are found at the second BRCT repeat.

We investigated the intramolecular interactions of BRCT-wt based on the previously determined[6] crystal structure and the changes caused by the individual mutations, as described in the materials and methods. Generally, it should be noted that only minor changes were identified at the level of H-bonds and ion-pairs.

Probing the thermal unfolding of BRCT variants by CD spectroscopy

Early CD spectroscopy studies on the thermal unfolding of BRCT-wt at various pH and buffer conditions provided evidence that the thermally denatured state of BRCT-wt retains most of the structural features of the native state.[25] Our current results with the five BRCA1 variants studied here are illustrated in Figure 2. From all it is clear that all the CD far-UV spectra of all variants perfectly overlap with the corresponding spectra of the BRCT-wt.

Comparing the spectra of the native and denatured states, it appears that the heat-induced alterations of the secondary structure elements in the native states are small (less than 6% loss in helical structure). Even if all the variants affect the thermal stability of BRCT, the secondary structure did not appear significantly influenced. In addition, the near-UV CD spectra of all the denatured states for the five BRCT variants were also determined and are identical to those of the BRCT-wt.

At various temperatures higher than the denaturation temperature, no changes in the CD spectra the five mutants are observed. These results are significant, since no CD-detectable protein aggregation takes place at pH 9.0.

Probing the thermal unfolding of the BRCT variants by DSC

Two important factors limit the thermodynamic investigation of heat-induced denaturation of BRCT-wt[31]: a) the pH-dependent aggregation in the thermally denatured state can severely distort the shape of the DSC thermal unfolding peaks that show nonreversibility, and b) the oligomerization of BRCT-wt in the native state is buffer-sensitive. Both factors may complicate the calorimetric result analysis.[25,31] A pH and buffer screening was performed to optimize the quality of the experimental data and to carry out the measurements of the BRCT variants studied. The suitable experimental conditions for the thermal unfolding of BRCT and its variants are 5 m*M* Na-borate pH 9.0, 200 m*M* NaCl (buffer D). High performance gel filtration chromatography experiments reveal that in this buffer, BRCT-wt and the five variants are all in a monomeric native state, as described in 3.3. A feature of this buffer is that its capacity is relatively temperature-independent, allowing for a direct comparison of the calorimetric results without incorporating unpredictable effects induced by pH variations.

The high-accuracy DSC results for BRCT-wt and variants under these conditions are presented in Table I. The heat capacity ($<\Delta Cp>$) versus temperature (T) profiles for the thermal denaturation of BRCT-wt are described by a single endothermic, irreversible peak (see Fig. 3) at $T_m = 48.3 \pm 0.5$°C, measured at a heating scan rate $u = 1.5$ K/min. The DSC profile is irreversible, and rate-dependent measurements reveal that the denaturation process is characterized by a slow irreversible step. Thus, the data obtained at the highest possible DSC scan rates are likely to exhibit limited kinetic distortion. In agreement with the gel filtration chromatography results, there is no dependence between T_m and the concentra-

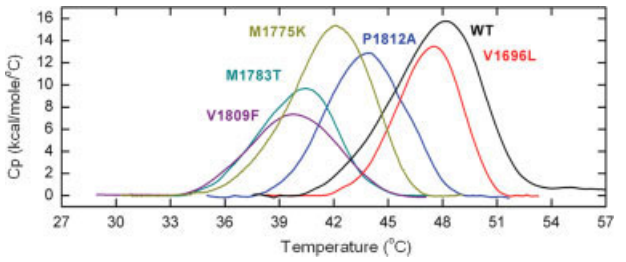

Figure 3

DSC profiles for the thermally induced denaturation of BRCT-wt and of five missense variants V1809F, M1783T, M1775K, P1812A, and V1696L. All profiles were obtained at pH 9.0, 5 m*M* Na-borate buffer, 200 m*M* NaCl and DSC heating rate $u = 1.5$ K/min. The concentration for all DSC thermograms was $C_t = 0.3$ mg/mL.

tion C_t, confirming that native BRCT-wt as well as the five mutants are in a monomeric state.

The BRCT mutants V1696L, M1775K, M1783T, V1809F, and P1812A were investigated according the conditions established for the BRCT-wt. In all cases, the DSC thermograms for the heat denaturation were obtained at $u = 1.5$ K/min in buffer D. For the five mutants studied, the thermal denaturation of the BRCT variants was irreversible and adequately free from aggregation-induced distortions. Calorimetric results obtained for different C_t values are presented in Table I. For the protein concentrations $C_t = 0.3$ and 0.4 mg/mL used, the calorimetrically-measured thermal unfolding enthalpy $(\Delta H)_{cal}$ and T_m values were found to be independent of C_t.

Comparing the calorimetric results of M1775K and V1809F to those for BRCT-wt, it can readily be deduced that $(\Delta H)_{cal}$ and T_m are affected. $(\Delta H)_{cal}$ is lower than the corresponding enthalpic content for the denaturation of BRCT-wt, and T_m exhibits a very significant decrease, by almost 6°C.

In contrast, $(\Delta H)_{cal}$ obtained for V1696L is comparable with BRCT-wt, while the T_m are also very similar.

Of particular interest is the mutant P1812A. Comparison of the calorimetric results of P1812A mutant with BRCT-wt and other studied BRCT mutations, leads to the conclusion that $(\Delta H)_{cal}$ and T_m are restrictly affected. $(\Delta H)_{cal}$ is lower than the corresponding enthalpic content for the denaturation of BRCT-wt, and T_m exhibits a downward shift by almost 4°C. Finally, the (ΔH)cal and T_m of M1783T are considerably lower compared to BRCT-wt.

In vitro interactions of BRCT-wt and variants with the phosphorylated binding sites of BACH1/BRIP1 (pBACH1/BRIP1) and CtIP (pCtIP) as determined by ITC

The interaction parameters of the BRCT-wt and the five missense variants with pBACH1/BRIP1 and pCtIP were determined by employing ITC, as described in the materials and methods. The ITC experimental data were analyzed via nonlinear least square fits of the integrated heat per injection versus molar ratio to a single-site binding model. The fitting results of the binding experiments for the affinity of the interaction (K_a) and the measurable heat as enthalpy (ΔH) of BRCT-wt and the five mutants, for pBACH1/BRIP1 and pCtIP, respectively, are summarized in Table II. For comparison, the Table also includes three previously published[25] mutants, marked with (*).

From the data presented in Table II and the ITC graphs illustrated in Figure 4, the following conclusions can be drawn: (a) BRCT-wt binds to both pBACH1/BRIP1 and pCtIP, with binding parameters identical to those previously published, (b) in all cases thermally denatured proteins showed no binding, (c) the mutants M1783T and P1812A were found to bind to both phosphopeptides analogously to what was found for the previously published V1833M mutant, (d) the mutant V1696L binds only to pBACH1/BRIP1, albeit with a binding affinity ~10 times lower than the corresponding for BRCT-wt, (e) the mutants M1775K and V1809F do not show binding to either pBACH1/BRIP1 or to pCtIP, as previously reported[25] for the missense variants M1775R and R1699W.

Structural properties of BRCT-wt and mutants in complex with pBACH1/BRIP1 and pCtIP

The atomic interactions of BRCT with phosphopeptides, pBACH1/BRIP1 and pCtIP, were analyzed by

Table II

Binding Parameters of BRCT-wt and Mutants

Mutants	N	K_a ($\times 10^6$ M^{-1})	ΔH (kcal/mol)
Binding to BACHI/BRIP1 (a)			
BRCT-wt	0.96	5.89 ± 0.53	17.2 ± 0.4
V1696L	1.10	0.48 ± 0.08	12.9 ± 0.3
M1775K		No Binding	
M1783T	0.90	4.10 ± 0.40	13.4 ± 0.2
V1809F		No Binding	
P1812A	1.14	1.38 ± 0.20	17.4 ± 0.4
M1775R*		No Binding	
R1699W*		No Binding	
V1833M*	0.94	3.72 ± 0.50	16 ± 0.3
Denatured molecules		No Binding	
Binding to CtIP (b)			
BRCT-wt	0.96	0.76 ± 0.13	10.90 ± 0.3
V1696L		No Binding	
M1775K		No Binding	
M1783T	0.90	0.67 ± 0.04	11.8 ± 0.3
V1809F		No Binding	
P1812A	1.10	0.40 ± 0.04	14.75 ± 0.4
M1775R*		No Binding	
R1699W*		No Binding	
V1833M*	1.04	1.43 ± 0.17	11.6 ± 0.3
Denatured molecules		No Binding	

(a) pBACHI/BRIP1 and (b) pCtIP phosphopeptides.

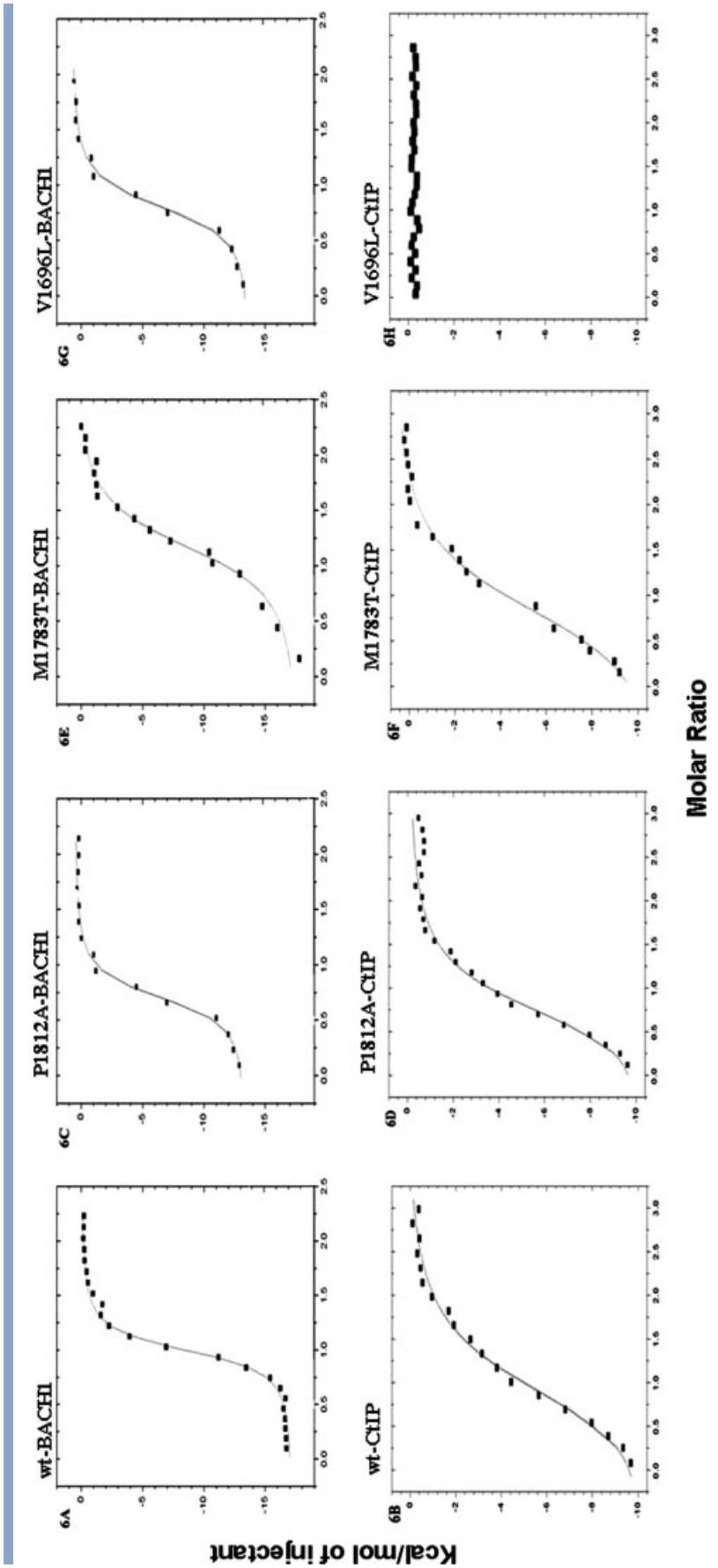

Figure 4

The interactions of BRCT-wt as well as the variants P1812A, M1783T, V1696L with the BACH1/BRIP1 and CtIP phosphopeptides. The isothermal plots were obtained at 20°C in pH 9.0, 5 m*M* Na-borate buffer, 200 m*M* NaCl. Figures: 6A. BRCT-wt-BACH1/BRIP1 binding, 6B. BRCT-wt-CtIP binding, 6C. P1812A-BACH1/BRIP1 binding, 6D. P1812A-CtIP binding, 6E. M1783T-BACH1/BRIP1 binding, 6F. M1783T-CtIP binding, 6G. V1696L-BACH1/BRIP1 binding, 6H. V1696L-CtIP, no binding observed. The fitting results are presented in Table II. The data presented are normalized, integrated heat data (*y* axis) (Kcal/mol of injectant) versus molar ratio (*x* axis). The baseline of the exothermic heat pulses (raw data, not shown), as well as the peptide dilution heats have been subtracted.

Table III
Residues of BRCA1-BRCT Involving Inter-Atomic Interactions with pBACH1/BRIP1, pCtIP and the Selected Mutations with Potential Hydrophobic Effect on the Protein Complexes

BRCT-pBACH1/BRIP1 Complex		
BRCA1-BRCT residues	pBACH1/BRIP1 residues (ISRSTpSPTFNKQ)	Mutations with potential hydrophobic effect
Glu1698	Ile1	V1696L
	Ser2	
Lys1702	pSer6	R1699W,V1696L
Thr1700	Thr8	V1696L,R1699W
Met1775	Phe9	M1775K,V1809F,M1775R
Val1740		V1696L
Arg1699		V1696L,R1699W
Val1741	Asn10	M1775K,M1775R
Asp1813	Gln12	P1812A
BRCT-pCtIP Complex		
BRCA1-BRCT residues	pCtIP residues (PTRVSpSPVFGAT)	Mutations with potential hydrophobic effect
Lys1702	pSer6	R1699W, V1696L
Met1775		M1775K,V1809F,M1775R
Val1740	Phe9	V1696L
Arg1699		V1696L,R1699W

employing the WHATIF and PYMOL protein analysis programs previously described. We used these data to explore the influence of the five individual mutations of BRCT and these interactions to interpret our experimental data. The obtained results are summarized in Table III.

Currently published structural studies of BRCT wt or other mutants reveal the crucial role of specific residues on the protein's interaction. Ser1655, Gly1656, and Lys1702 interact with pSer6 of both pBACH1/BRIP and pCtIP proteins.[16,17,23] Furthermore, hydrophobic intermolecular interactions were confirmed between Met1775 and Val1740 as well as between the hydrogen bonds of Arg1699 with Phe9 of both pBACH1/BRIP and pCtIP.[16,17]

Briefly, the BRCT-pBACH1 complex shows over 25 interatomic interactions. These interactions involve Ser4, pSer6, Thr8, Phe9, and Asn10 residues of pBACH1/BRIP1 and Leu1657, Ser1655, Thr1700, Val1741 of BRCT.[16]

The side chain of Phe9 of pBACH1/BRIP1 interacts with methyl groups of Leu1839 and the aromatic ring of Phe1704, and the methyl group of Leu1839 is crucial for both interactions. Furthermore, the Ser4, pSer6, Thr8, Phe9, and Asn10 amino acids of pBACH1 interact with Leu1657, Ser1655, Thr1700, Val1741 of BRCT, and the Thr8, Thr1700 contact may specify the contribution of both residues and the specific role of Thr8 (pSer +2) on molecular interactions, based on protein structure database. Stabilizing hydrogen bonds are reported for Lys1698, Asp1813 with Ser2, Gln12, and Gly1656 with Arg3, Ser4 of phosphopeptide (see Fig. 5).[16]

Based on the crystal structure of the BRCT-pCtIP complex, hydrophobic interactions between V1740 and M1775 have been found, in addition to the hydrogen bond network between Ser1655, Gly1656, Lys1702 and pSer and between R1699 and Phe9. Furthermore, weak Van der Waals forces between Val14, Pro7, and Gly10 of pCtIP and BRCT residues have also been described.[17]

A direct comparison of the residues involved in the interatomic interactions of both peptides reveals the differences in binding affinities of BRCT-pBACH1/BRIP1 in contrast with those of pCtIP. The Ser4 of pBACH1/BRIP1 interact via hydrogen bonds with Gly1656 in contrast with Val4 of pCtIP, which interact by hydrophobic interactions with Leu1657 by removing the phosphopeptide from the binding pocket. In addition, the hydrogen bonds of Asn10 and Gln12 with Arg1699, Asp1813 and salt bridges of Lys11 with Glu1863 and Asp1840 are crucial for the interaction of BRCT-pBACH1/BRIP1 and do not appear in the BRCT-pCtIP complex.[16,17]

The selected studied mutations are structurally located near those BRCT residues crucial for the interatomic interactions of both phosphopeptides, such as Glu1698, Arg1699, and V1740 (close to V1696), Asp1813 (close to P1812), L1780 (close to V1809F), or are involved in hydrophobic interactions and hydrogen bonds such as M1775, R1699. Moreover, M1783T and V1833M seem to be less involved in interatomic interacting rearrangements.

DISCUSSION

Based on worldwide genetic screening data, missense mutations at the BRCT domain of human BRCA1, which have been argued to be associated with predisposition to hereditary breast/ovarian cancer, were selected for extended protein analysis. These mutants are M1775K, V1809F, P1812A, M1783T, and V1696L. The five BRCT variants carrying the respective single amino acid mutations have been selected here for extended protein analysis. They were produced as recombinant proteins in *E. coli*, prepared in high purity and characterized for their structural integrity, thermal stability and binding capacity to the BACH1/BRIP1 and CtIP phosphopeptides, by employing CD, high-accuracy DSC and ITC respectively. The mutation-induced structural alterations have been modeled based on the published X-ray structure of BRCA1-BRCT as well as on the structures of BRCA1-BRCT complexes with pBACH1/BRIP1 and pCtIP. The potential intra- and intermolecular changes caused by the point mutations are summarized in Table III in the "Results" section.

Based on their location, the selected mutations cover the crucial regions of the BRCT domain. One mutation is located at the N-terminal BRCT repeat (V1696L), another two, M1783T and M1775K, are at the inter-repeat interface region directly affecting the BACH1/

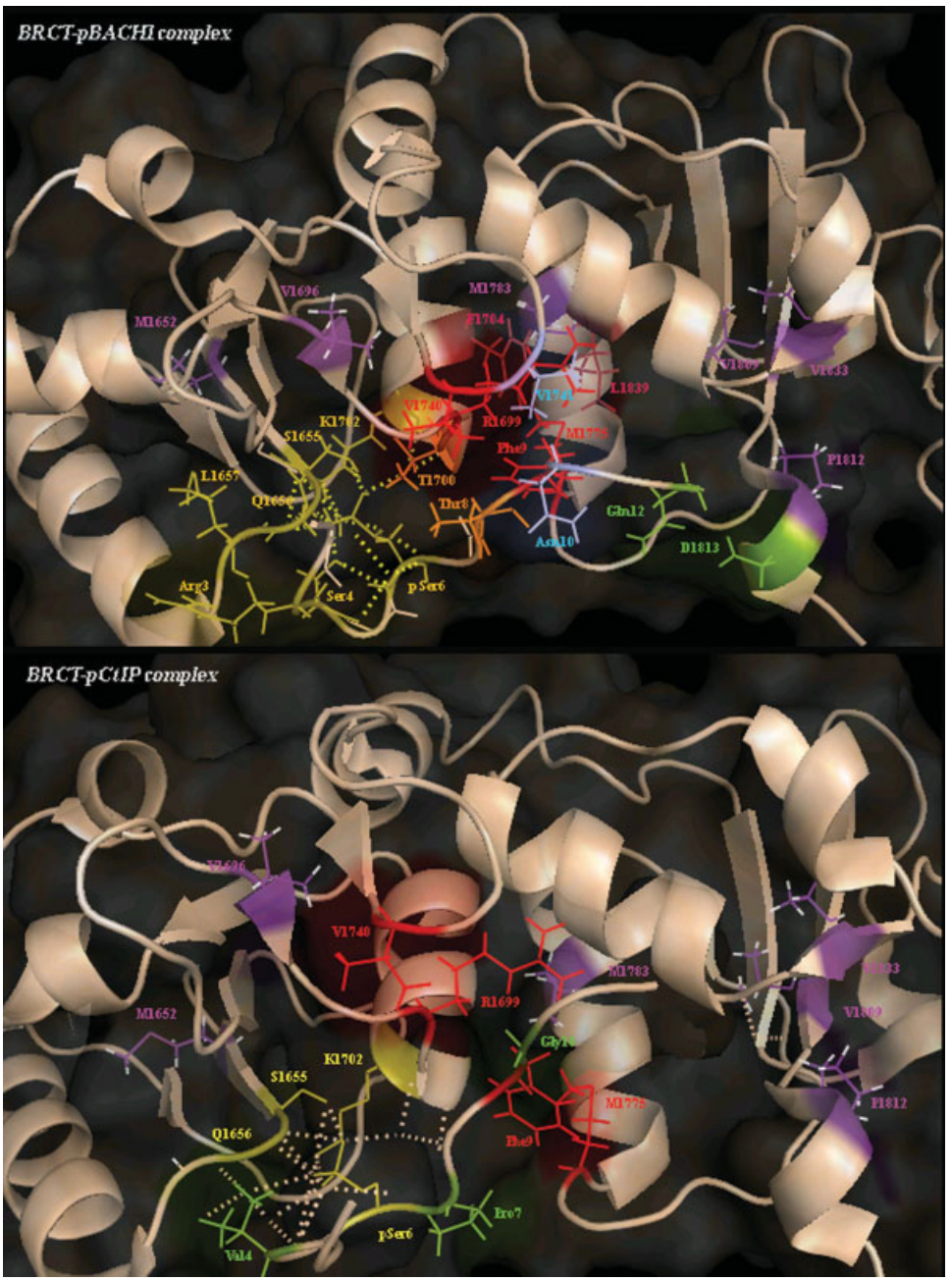

Figure 5

Intermolecular interaction of BRCA1-BRCT with phosphopeptides pBACH1/BRIP1 and pCtIP. The position of the selected mutants and the residues participating at interatomic interactions can be observed. Ser1655, Gly1656, and Lys1702 interact with pSer6. Hydrophobic intermolecular interactions between Met1775 and Val1740 and hydrogen bonds of Arg1699 with Phe9 of both pBACH1 and pCtIP were determined.[16,17] In the case of BRCT-pBACH1/BRIP1, complex interatomic interactions were specified involving the Ser4, pSer6, Thr8, Phe9, and Asn10 residues of pBACH1/BRIP1. These residues also interact with Leu1657, Ser1655, Thr1700, Val1741 of BRCT, and the Thr8, Thr1700 contact may specify the contribution of both residues and the specific role of Thr8 (pSer +2) on the molecular interactions. In the previous[16] published interactions of Ser1655, Gly1656, Lys1702 with pSer6, the hydrogen bonds of R1699 with Phe9 and the hydrophobic of V1740 and M1775 between BRCA1-BRCT and both phosphopeptides, further Van der Waals forces between Val4, Pro7, Gly10 of pCtIP and BRCT residues have also been described.[17] [Color figure can be viewed in the online issue, which is available at www.interscience.wiley.com.]

BRIP1 and CtIP phosphopeptide binding pocket, and the last two V1809F and P1812A are located at the C-terminal BRCT repeat. In accordance with previously reported findings, the calorimetric results reported here support the scenario that thermal unfolding mechanisms mainly involve the hydrophobic inter-BRCT-repeat interface, while CD-based structural comparisons do not reveal structural alterations in the secondary or tertiary struc-

ture of the mutants.[31] The obtained results comprise a framework, combining thermodynamic, structural and binding affinity data, for comparative studies of the various mutants in an attempt to elucidate the role of pathogenic mutations on function mechanisms and tumorigenesis. A discussion of the effects of each individual mutation studied here follows.

Met1775 to Lys mutation

M1775K is a rare breast cancer-linked mutation. It has been identified only in two unrelated families of European ancestry with a history of breast cancer.[31] Met1775 is located at the inter-BRCT-repeat interface and is well conserved among the currently available BRCA1-BRCT domain orthologs.[26] Met1775 is strongly involved in the phosphopeptide-binding pocket of the BRCT domain. Another mutation of Met1775, namely the mutation M1775R, is much more frequent worldwide among patients with hereditary breast/ovarian cancer, its association with the disease is epidemiologically established and was first characterized to be linked to cancer.[1,32,33] The mutant M1775R has already been thoroughly studied structurally[26] as well as biophysically[34,25] and no interaction with either pBACH1/BRIP1 or pCtIP has been shown.

Direct comparisons between the crystal structures of the BRCT-pBACH1 and BRCT-pCtIP complexes and the structure of variant M1775R demonstrated that the replacement of Met1775 with Arg blocks access of the peptide- Phe9 (Phe993 for pPBACH1 and Phe330 for pCtIP) to the hydrophobic inter-BRCT-repeat groove. Moreover, since Met1775 is part of the hydrophobic contact surface between the two BRCT repeats and is packed within a predominantly hydrophobic pocket near the edge of the inter-repeat interface, substitution of this residue with an Arg would extrude the mutated side-chain form the hydrophobic core, inducing charge–charge repulsion and the rearrangement of the hydrogen-bond network at the inter-BRCT interface, eventually destabilizing the native fold.[26] This has been evidenced experimentally by reported stability measurements via thermal and chemical denaturation.[25,34]

The M1775K missense variant fails to bind to either pBACH1/BRIP1 or pCtIP.[35] Structural analysis of the interatomic interactions of Lys1775 show a direct clash of its side chain with Phe +3 of either phosphopeptide, a result arising from the disruption of the BRCT-phosphopeptide binding pocket. From the calorimetric results reported here it becomes obvious that M1775K also affects stability, albeit not as severely as M1775R does. The differences can be attributed to the different length and charge of the Arg and Leu side chains. The combination of ITC and DSC results corroborate previously reported multimodal findings that the mutation M1775K is pathogenic.[35]

Met1783 to Thr mutation

The M1783T mutation has been reported in African, Latin American and Western European families (BIC). The intermediate protease sensitivity of this mutation results from combined deleterious effects of protein core cavitation and the burial of a polar hydroxyl group at the BRCT interface.[36] Met1783 is located at the conserved triple-helical interface of the C-terminal BRCT repeat in the vicinity of the Phe binding pocket for pBACH1/BRIP1 and pCtIP. Apparently, substitution of Met1783 with Thr does not structurally alter the +3 Phe binding groove since the ITC results reported here compare well to those obtained for BRCT-wt. In fact, by comparing the measured binding constant K_a, for the interaction with pBACH1/BRIP1 (M1783T 4.1 $\times$ 10^6 M^{-1} vs. 5.89 $\times$ 106 M^{-1} for BRCT-wt) as well as with pCtIP (M1783T 0.67 $\times$ 10^6 M^{-1} vs. 0.76 $\times$ 10^6 M^{-1} BRCT-wt with) it can straightforwardly be concluded that M1783T does not significantly affect these interactions.

The CD experiments reported here reveal that the M1783T mutant is not structurally different from the wild-type. Nevertheless, at the atomic level the mutated Thr1783 interacts via hydrogen bond formation with Gly1779 and Leu1786 but not with Cys1787, like Met1783 does. In addition, Thr1783 may possibly alter the interatomic contacts with Val1838, Val1842, and Leu1839.

Thus, even if the M1783T mutant's binding affinity to either phosphopeptide is not remarkably affected compared with BRCT-wt, the intramolecular rearrangements can destabilize the overall native fold. This is demonstrated by the severe reduction of T_m as well as of $(\Delta H)_{cal}$ values obtained from the heat-induced denaturation experiments (Table I). $\Delta(\Delta H)$ (the difference between ΔH of the wtBRCT and ΔH of the mutant) is 33 kcal/mol which is considerably larger compare to all the other mutants studied here. This is in agreement with previously published studies of the thermodynamic consequences for the substitutions of the buried hydrophobic amino acid with the polar one.[37] An analogous situation, albeit with more significant effects concerning the binding constants, has been reported for the V1833M mutant.[25] As for V1833M, the characterization of M1783T as pathogenic may be considered premature, based on the experimental evidence presented here.

Val1809 to Phe mutation

V1809F is a rare mutation linked to hereditary breast/ovarian cancer since, to date, only four cases of the mutation have been submitted to the BIC database. Even if it is apparently distant from the Phe +3 binding pocket, crystal structure analyses of variant V1809F revealed that the substitution of Val at position 1809 with the bulkier Phe side chain influences the intramo-

lecular hydrophobic interactions with Val1838, Trp1837, and Leu1780. It is rather the interaction of Phe1809 with Leu1780 which will likely lead to an adjustment of the latter's side chain, which in turn can be accommodated by a rearrangement of the neighboring Met1775 side chain, bearing a significant effect upon the structure of the Phe +3 binding pocket (see Fig. 5).[34,36] This, of course, can explain the *in vitro* loss of function reported here, as far as the interactions with pBACH1/BRIP1 and pCtIP are concerned. The residue Val1809 is conserved among species.[36] Val1809, like Met1775, is crucial for the integrity of phosphopeptide binding pocket and thus the studied mutation exhibits no binding to either pBACH1/BRIP1 or pCtIP phosphopeptides.

Moreover, the mutant V1809F appears to be severely destabilized with respect to BRCT-wt. The thermodynamic results reported here for the heat induced denaturation of the molecule demonstrate a severe drop in the values of T_m and $(\Delta H)_{cal}$ analogous to those encountered for the mutant M1775R.[25] Apparently, the Val to Phe substitution at position 1809, even though it concerns the substitution of a non polar amino acid by another non polar one, destabilizes the overall native fold, most likely due to the disruption of the hydrogen-bond network leading to a destabilization of the hydrophobic inter-BRCT repeat interface.

The effects of mutation V1809F are major. Even though CD results show no structural alterations of the mutant compared to the BRCT-wt, the combination of loss-of-function with the destabilization of the native fold in a way analogous to mutation M1775R strongly supports arguments classifying V1809F as pathogenic.

Pro1812 to Ala mutation

The mutation P1812A has already been reported in Ashkenazi Jews as well as in Greek families with familial breast cancer.[2,38,39] As for Val1809, the residue Pro1812 is well conserved among species,[36] and being located at the C-terminal BRCT-repeat is important for the structural integrity of the Phe +3 binding pocket, even though it is not one of the residues forming it. Substitution of Pro1812 to Ala affects the interatomic interactions and the local hydrogen bond network, albeit not as severely as the mutation V1809F does. While the variant P1812A does bind to the BACH1/BRIP1 and CtIP phosphopeptides, both the binding affinities as well as the stability of the mutant are affected. For the interaction with pBACH1/BRIP1, a direct comparison of K_a for the P1812A and BRCT-wt indicates a major decrease for the former (1.38 and 5.89, respectively), while the K_a for binding to pCtIP is 0.4 versus 0.76 for the BRCT-wt. The calorimetric results are also affected, indicating a significant decrease in T_m. The $\Delta(\Delta H)$ values relative to BRCT-wt, is 14 kcal/mol, which is not as significant as for the $\Delta(\Delta H)$ for M1783T, not surprising since the P1812A substitution involves two hydrophobic amino acids.[37]

Even though the mutation P1812A is frequently encountered in families with a history of breast/ovarian cancer, the biophysical findings reported here, while indicative of a deviation from wild-type behavior, are not sufficient to characterize this mutation as pathogenic.

Val1696 to Leu mutation

Only one case of this mutation has been reported in the BIC database. The residue Val1696 is exposed to the solvent since it is located at the surface of the N-terminal BRCT repeat, right at the loop connecting the β_3-sheet and the α_2-helix. It confers moderate protease susceptibility to the BRCT domain.[34] This loop forms an extended hairpin structure, participates in the formation of one of the two conserved BRCT surfaces targeted by missense mutations, and may be the primary site of interaction with the BRCA1-associated helicase pBACH1/BRIP1.[34,36] The ITC results presented here reveal that the replacement of Val at position 1696 with Leu abolishes the binding of the BRCT domain to pCtIP, while the binding to pBACH1 has been severely altered (K_a ratio between BRCT-wt/BRCT-V1696L = 12.3). Both effects may be due to a local destabilization that causes disruption of molecular contacts. Indeed, Leu1696 interacts via hydrogen bonds with Val1740, a residue which is involved in the intermolecular hydrophobic interaction with Phe9 of the pBACH1/BRIP1 as well as of the pCtIP peptides. In the case of the pCtIP interaction, these hydrophobic rearrangements may explain the complete abolition of the binding of the V1696L mutant. On the other hand, in the case of the pBACH1/BRIP1 interaction, the additional hydrogen bonds of G1698 and V1741 with Ile1, Ser2, Asn10 will promote the binding ability, albeit with a much lower affinity than for the wt (see Fig. 5).

The experimental results presented here provide a comparative measure of the effects of missense mutations of the BRCA1-BRCT domain upon the structural, calorimetric and as well as the interaction-thermodynamics concerning the binding with the BACH1/BRIP1 and CtIP phospopeptides. Point mutations do not affect the mutants' secondary and tertiary structure characteristics. They can influence the integrity of the Phe +3 binding groove, thus affecting the enthalpically-driven binding ability with pBACH1/BRIP and pCtIP, as evidenced by ITC-measured calorimetric parameters. Furthermore, point mutations can destabilize the overall native fold by affecting the intramolecular interactions in the general area of the hydrophobic inter-BRCT-repeat interface with direct measurable effects upon the values of the DSC-measured calorimetric parameters. According to previous published studies the single amino acid substitutions seem to be crucial for protein stability.[37] Burial of polar

groups in the nonpolar interior of a protein is highly destabilizing particularly increasing the enthalpy change. The degree of destabilization depends on the relative polarity of this group. Additionally, the destabilizing effect of dehydration of polar groups upon burial can be neutralized or compensated if these buried polar groups form hydrogen bonding.[37]

Furthermore for the mutations studied here, M1775K and V1809F alter the binding site as well the stability of the molecule and are most likely pathogenic. M1783T and P1812A only affect the mutant's stability but bear no effect upon the binding capacity. As it has recently been shown the interaction of BRCA1-BRCT with phosphorylated peptides involves two binding conformations of the BRCT domain.[40] Stability issues may thus alter the conformational balance in solution and in turn affect the domain's function. Finally, V1696L poses an interesting problem since, being a surface mutation, it has no effect upon the stability while the binding ability is affected in the case of pBACH1/BRIP1 and is fully abolished in the case of the pCtIP interaction.

ACKNOWLEDGMENTS

The authors thank Dr. D. Yannoukakos for his scientific advice and Dr. C. Zikos for the synthesis of the phosphopeptides. Experimental assistance from A. Thanassoulas and Dr. G. Nikolopoulos is acknowledged as well as the use of the facilities of the Centre for Crystallographic Studies of Macromolecules of NCSR "Demokritos". The data processing was performed on Mac OS X.

REFERENCES

1. Futreal PA, Liu Q, Shattuck-Eidens D, Cochran C, Harshman K, Tavtigian S, Bennett LM, Haugen-Strano A, Swensen J, Miki Y. BRCA1 mutations in primary breast and ovarian carcinomas. Science 1994;224:120–122.
2. Ferla R, Calo V, Cascio S, Rinaldi G, Badalamenti G, Carreca I, Surmacz E, Colucci G, Bazan V, Russo A. Founder mutations in BRCA1 and BRCA2 genes. Ann Oncol 2007;6:93–98.
3. Brose MS, Rebbeck TR, Calzone KA, Stopfer JE, Nathanson KL, Weber BL. Cancer risk estimates for BRCA1 mutation carriers identified in a risk evaluation program. J Nat Cancer Inst 2002;9418: 1365–1372.
4. Robles-Diaz L, Goldfrank DJ, Kauff ND, Robson M, Offit K. Hereditary ovarian cancer in Askenazi Jews. Fam Cancer 2004;3:259–264.
5. Antoniou A, Pharoah PD, Narod S, Risch HA, Eyfjord JE, Hopper JL, Loman N, Olsson H, Johannsson O, Borg A, Pasini B, Radice P, Manoukian S, Eccles DM, Tang N, Olah E, Anton-Culver H, Warner E, Lubinski J, Gronwald J, Gorski B, Tulinius H, Thorlacius S, Eerola H, Nevanlinna H, Syrjäkoski K, Kallioniemi OP, Thompson D, Evans C, Peto J, Lalloo F, Evans DG, Easton DF. Average risks of breast and ovarian cancer associated with BRCA1 or BRCA2 mutations detected in case series unselected for family history: a combined analysis of 22 studies. Am J Hum Genet 2003;72:1117–1130.
6. Williams RS, Green R, Glover JN. Crystal structure of the BRCT repeat region from the breast cancer associated protein BRCA1. Nat Struct Biol 2001;10:838–842.
7. Joo WS, Jeffrey PD, Cantor SB, Finnin MS, Livingston DM, Pavlretich NP. Structure of the 53BP1 BRCT region bound to p53 and its comparison to the BRCA1 BRCT structure. Genes Dev 2002;16:583–593.
8. Stenson PD, Ball EV, Mort M, Phillips AD, Shiel JA, Thomas NS, Abeisighe S, Krawczak M, Cooper DN. Human gene mutation database (HGMD). Hum Mutat 2003;21:577–581.
9. Merajver SD, Pham TM, Caduff RF, Chen M, Poy EL, Cooney KA, Weber BL, Collins FS, Johnston C, Frank TS. Somatic mutations in the BRCA1 gene in sporadic ovarian tumours. Nature Genet 1995; 9:439–443.
10. Rodriguea JA, Au WW, Henderson BR. Cytoplasmic mislocalization of BRCA1 caused by cancer associated mutations in the BRCT domain. Exp Cell Res 2004;293:14–21.
11. Scully R, Ganesan S, Brown M, De Caprio JA, Cannistra SA, Feunteun J, Schnitt S, Livingston DM. Location of BRCA1 in human breast and ovarian cancer cells. Science 1996;272:123–126.
12. Wilson CA, Ramos L, Vilasenor M, Andres KH, Press MH, Clarke K, Karlan B, Chen JJ, Scully R, Livingston D, Zuch RZ, Kanter MH, Cohen S, Calzone F, Slamon D. Localization of human BRCA1 and its loss in high grade non inherited breast carcinomas. Nature 1999;21:236–241.
13. Mirkovic N, Marti-Remon MA, Weber BL, Sali A, Monteiro NA. Structure based assessment of missense mutations in human BRCA1: Implications for breast and ovarian cancer predisposition. Cancer Res 2004;64:3790–3797.
14. Ray H, Moreau K, Dizin E, Callebaut I. ACCA phosphopeptide recognition by the BRCT repeats of BRCA1. J Mol Biol 2006;359:973–982.
15. Derbyshire DJ, Basu BP, Serpell LC, Joo WS, Date T, Iwabuchi K, Doherty AJ. Crystal structure of human 53BP1 BRCT domains bound to p53 tumour suppressor. EMBO J 2002;21:3863–3872.
16. Botuyan MV, Nomine Y, Yu X, Juranic N, Macura S, Chen J, Mer G. Structural basis of BACH1 phosphopeptide recognition by BRCA1 tandem BRCT domains. Structure 2004;24:1137–1146.
17. Varma AK, Brown RS, Birrane G, Ladias JA. Structural basis for cell cycle checkpoint control by the BRCA1-CtIP complex. Biochemistry 2005;44:10941–10946.
18. Kumaraswamy E, Shiekhattar R. Activation of BRCA1/BRCA2-associated helicase BACH1 is required for timely progression through S phase. Mol Cell Biol 2007;19:6733–6741.
19. Clapperton JA, Manke IA, Lowery DM, Ho T, Haire LF, Yaffe MB, Smerdon MB. Structure and mechanism of BRCA1 BRCT domain recognition of phosphorylated BACH1 with implications for cancer. Nat Struct Mol Biol 2004;11:512–518.
20. Chinnadurai G. CtIP, a candidate tumor susceptibility gene is a team player with luminaries. Biochim Biophys Acta 2006;1765:67–73.
21. Hammet A, Magill C, Heierhorst J, Jackson SP. Rad9 BRCT domain interaction with phosphorylated H2AX regulates the G1 checkpoint in budding yeast. EMBO Rep 2007;8:851–857.
22. Shiozaki EN, Gu L, Yan N, Shi Y. Structure of the BRCT repeats of BRCA1 bound to a BACH1 phosphopeptide: implications for signaling. Mol Cell 2004;14:405–412.
23. Williams RS, Lee MS, Hau DD, Glover JN. Structural basis of phosphopeptide recognition by the BRCT domain of BRCA1. Nat Struct Mol Biol 2004;14:519–525.
24. Yu X, Chen J. DNA damage-induced cell cycle checkpoint control requires CtIP, a phosphorylation-dependent binding partner of BRCA1 C-terminal domains. Mol Cell Biol 2004;24:9478–9486.
25. Nikolopoulos G, Pyrpassopoulos S, Thanassoulas A, Klimentzou P, Zikos C, Vlassi M, Vorgias CE, Yannoukakos D, Nounesis G. Thermal unfolding of BRCA1-BRCT variants. Biochim Biophys Acta 2007;6:772–780.
26. Williams RS, Glover JN. Structural consequences of a cancer-causing BRCA1-BRCT missense mutation. J Biol Chem 2003;278:2630–2635.
27. Laemmli UK. Cleavage of structural proteins during the assembly of the head of bacteriophage T4. Nature 1970;227:680–685.

28. Robinson DW, Bradford GE. Cellular response to selection for rapid growth in mice. Growth 1969;33:221.
29. Stanley G, Hippel PH. Calculation of protein extinction coefficients from amino acids sequence data. Anal Biochem 1989;2:319–326.
30. Pace N, Valdos F, Fee L, Grimsley G, Gray T. How to measure and predict the molar absorption coefficient of a protein. Protein Sci 1995;4:2411–2423.
31. Pyrpassopoulos S, Ladopoulou A, Vlassi M, Papanikolau Y, Vorgias CE, Yannoukakos D, Nounesis G. Thermal denaturation of the BRCT tandem repeat region of human tumour suppressor gene product BRCA1. Biophys Chem 2005;114:1–12.
32. Deffenbaugh AM, Frank TS, Hoffman M, Cannon-Albright L, Neuhausen SL. Characterization of common BRCA1 and BRCA2 variants. Genet Test 2002;6:119–121.
33. Humphrey JS, Salim A, Erdos M, Collins FS, Brody LC, Klausner RD. Human BRCA1 inhibits growth in yeast: potential use in diagnostic testing. Proc Natl Acad Sci USA 1997;11:5820–5825.
34. Williams RS, Chasman DI, Hau DD, Hui B, Lan AY, Glover JN. Detection of protein folding detects caused by BRCA1-BRCT truncation and missense mutations. J Biol Chem 2003;278:53007–53016.
35. Tischkowitz M, Hamel N, Carvalho MA, Birrane G, Soni A, Beers EH, Joosse SA, Wong N, Novak D, Quenneville LA, Grist SA, Nederlof PM, David E Goldgar DE, Tavtigian SV, Monteiro AN, Ladias JA, Foulkes W. Pathogenicity of the BRCA1 missense variant M1775K is determined by the disruption of the BRCT phopshpeptide binding pocket: a multi modal approach. Eur J Hum Genet 2008;7:820–832.
36. Mark Glover JN. Insights of the molecular basis of human hereditary breast cancer from studies of the BRCA1 BRCT domain. Fam Cancer 2006;5:89–93.
37. Loladze VV, Ermolenko DN, Makhatadze GI. Thermodynamic consequences of burial of polar and non-polar amino acid residues in the protein interior. J Mol Biol 2002;320:343–357.
38. Kaufman B, Laitman Y, Carvalho MA, Endelman L, Menachem TD, Zidan J, Monteiro AN, Friedman E. The P1812A and P25T BRCA1 and the 5164del4 BRCA2 mutations. Occurrence in high-risk non Askenazi Jews. Genet Test 2006;10:200–207.
39. Martinez-Ferrandis JI, Vega A, Chirivella I, Marin-Garcia P, Insa A, Lluch A, Carracedo A, Chaves FJ, Garcia-Condle J, Cervantes A, Armengod ME. Mutational analysis of BRCA1 and BRCA2 in Mediterranean Spanish women with early onset breast cancer: identification of three novel pathogenic mutations. Hum Mutat 2003;659:1–5.
40. Nomine Y, Botuyan V, Bajzer Z, Owen WG, Caride AJ, Wasielewski E, Mer G. Kinetic analysis of interaction of BRCA1 tandem breast cancer C-terminal domains with phosphorylated peptides reveals two binding conformations. Biochemistry 2008;47:9866–9879.